Quantized conductance through an asymmetric narrow constriction in a three-dimensional electron gas

Holger Waalkens
School of Mathematics, University of Bristol, University Walk, Bristol BS8 1TW, United Kingdom
(Received 14 May 2004; revised manuscript received 26 August 2004; published 24 January 2005)

The quantized ballistic transmission of a three-dimensional electron gas through a narrow constriction modeled by an asymmetric hyperboloid is studied. The conductance as a function of voltage jumps by integer multiples of $e^2/(\pi\hbar)$ each time a new transition channel opens in the plane of narrowest restriction, which has the shape of an ellipse. There are two different modes ("whispering gallery modes" and "bouncing ball modes") which lead to different conductance steps. The smoothing of the conductance steps is discussed in terms of phase space tunneling through a dynamical barrier. A comprehensive interpretation of the quantum mechanical results is obtained from relating them to the corresponding classical motions.

DOI: 10.1103/PhysRevB.71.035335 PACS number(s): 73.23.−b, 73.63.−b, 03.65.Sq

I. INTRODUCTION

Recent developments in experimental techniques have opened the way to study ballistic electron transport in a large number of so-called *mesoscopic systems* such as, e.g., quantum dots and quantum wires in semiconductor heterostructures,[1] metallic nanowires,[2,3] carbon nanotubes,[4] quantum corrals,[5] and even individual molecules.[6] These systems are typically on the fuzzy borderline between quantum mechanics and classical mechanics, and therefore offer an ideal testing ground for semiclassical theories which, e.g., lead to the explanation of the universality of conductance fluctuations.[7,8]

The geometry of the spatial confinement of the electron flow often involves one or several narrow constrictions or *point contacts*. A point contacts forms, e.g., if the tip of a scanning tunneling microscope is brought into contact with a metal surface.[9] Due to the strong spatial confinement, quantum effects are particularly strong at such points and can lead to a quantization of the conductance. Quantized conductance steps by integer multiples of the "elementary conductance" $e^2/(\pi\hbar)$ upon varying the applied voltage were first observed in quantum point contacts fabricated in semiconductor heterostructures by van Wees *et al.*[10] and Wharam *et al.*[11] Meanwhile they are a rather universal phenomenon, also observed in metal nanowires[2,3] and even liquid metals. Experiments by Rubio, Agraït, and Vieira,[12] and independently by Stalder and Dürig,[13] showed that on the formation of a nanoscale gold contact the conductance jumps are synchronized with cohesive force oscillations of the order of nanonewtons.

In this paper we consider the transmission between two three-dimensional electron reservoirs which are connected by a lead of the asymmetric hyperboloidal shape

$$\frac{x^2}{\tilde{c}^2}+\frac{y^2}{\tilde{b}^2}-\frac{z^2}{\tilde{a}^2}=1 \quad (\tilde{c}\geqslant\tilde{b}>0,\tilde{a}>0). \tag{1}$$

We employ a simple jellium model in which the electrons are assumed to move freely and to be confined to the hyperboloidal lead by a hard-wall potential. Utilizing semiclassical ideas, this model has been used, e.g., by Stafford *et al.*[14–16] to develop a theory of nanocohesion in metallic wires. The constriction (1) has a "bottleneck" in the x-y plane which is bounded by the ellipse $x^2/\tilde{c}^2+y^2/\tilde{b}^2=1$; see Fig. 1. The motivation for choosing constrictions of the type (1) is that they are the most general type of three-dimensional constriction for which the transmission problem can be separated and in this sense solved explicitly. This paper can thus be considered as a generalization of the two-dimensional transmission problem through a hyperbolic constriction studied by Yosefin and Kaveh.[17] The three-dimensional constrictions considered here include, e.g., the special case of axially symmetric constrictions studied by Torres, Pascual, and Sáenz.[18] The limiting case of a cylindrical constriction with an elliptic cross section will be discussed below in more detail.

We assume that the electrons are incident from the bottom ($z\ll-1$) and want to compute the transmission to the top ($z\gg1$). Following Landauer[19,20] and Büttiker[21] the conductance can be obtained from a scattering approach. For zero temperature the conductance for energy E is given by the Landauer-Büttiker formula

$$G(E)=\frac{e^2}{\pi\hbar}\sum_{n,m}|t_{nm}(E)|^2, \tag{2}$$

where $|t_{nm}(E)|^2$ is the transmission probability between the nth incoming mode and the mth outgoing mode for energy E. For a separable system there is no mode mixing, i.e.,

$$|t_{nm}(E)|^2=T_n(E)\delta_{nm}, \tag{3}$$

where δ_{nm} is the Kronecker symbol.

It is convenient to scale (x,y,z) by the semimajor axis $\tilde{c}$ of the bottleneck ellipse. Moreover, for an appropriate scaling of time and mass Planck's constant has the value 2π (i.e., $\hbar=1$) and the unit of energy becomes $\hbar^2/(\tilde{c}^2m_e)$ with m_e being the (effective) mass of the charge carriers. In order to compute the energy-dependent transmission probabilities T_n we have to find solutions of the free Schrödinger or Helmholtz equation

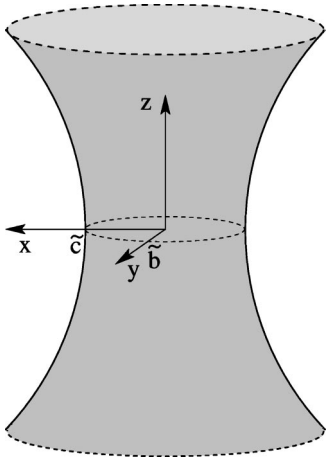

FIG. 1. Accessible region of a three-dimensional electron gas confined by the boundary hyperboloid (1).

$$-\frac{1}{2}\left(\frac{\partial^2}{\partial x^2}+\frac{\partial^2}{\partial y^2}+\frac{\partial^2}{\partial z^2}\right)\psi = E\psi \tag{4}$$

which for $z \gg 1$ are waves propagating in the positive z direction and satisfy Dirichlet boundary conditions, i.e., we require the restriction of ψ to the hyperboloid (1) to vanish. This defines a so-called *quantum billiard* which is open in the sense that there are no constrictions in z direction.

II. SEPARATION OF THE HELMHOLTZ EQUATION

The Helmholtz equation and, equally important, the boundary conditions can be separated in elliptic coordinates (ξ,η,ζ).[22,23] Each of them parametrizes a family of confocal quadrics

$$\frac{x^2}{s^2}+\frac{y^2}{s^2-b^2}+\frac{z^2}{s^2-a^2}=1, \tag{5}$$

where $s\in\{\xi,\eta,\zeta\}$, $b^2=1-\tilde{b}^2/\tilde{c}^2$, and $a^2=1+\tilde{a}^2/\tilde{c}^2$. For $s=\xi > a$ all terms in Eq. (5) are positive and the equation defines a family of confocal ellipsoids. Their intersections with the x-y plane, the x-z plane, and the y-z plane are planar ellipses with foci at $(x,y)=(\pm b,0)$, $(x,z)=(\pm a,0)$, and $(y,z)=(\pm(a^2-b^2)^{1/2},0)$, respectively. For $a>s=\eta>b$ the third term in Eq. (5) becomes negative. Equation (5) thus gives confocal one sheeted hyperboloids. Their intersections with the x-y plane are planar ellipses with foci $(x,y)=(\pm b,0)$; the intersections with the x-z plane and the y-z plane are planar hyperbolas with foci at $(x,z)=(\pm a,0)$ and $(y,z)=(\pm(a^2-b^2)^{1/2},0)$, respectively. For $b>s=\zeta>0$ the second and third terms in Eq. (5) are negative giving confocal two sheeted hyperboloids. Their intersections with the x-y plane and the x-z plane are planar hyperbolas with foci at $(x,y)=(\pm b,0)$ and $(x,z)=(\pm a,0)$, respectively; they do not intersect the y-z plane.

Inverting Eq. (5) within the positive (x,y,z) octant gives

$$x=\frac{\xi\eta\zeta}{ab}, \tag{6}$$

$$y=\frac{\sqrt{(\xi^2-b^2)(\eta^2-b^2)(b^2-\zeta^2)}}{b\sqrt{a^2-b^2}}, \tag{7}$$

$$z=\frac{\sqrt{(\xi^2-a^2)(a^2-\eta^2)(a^2-\zeta^2)}}{a\sqrt{a^2-b^2}} \tag{8}$$

with

$$0\leqslant\zeta\leqslant b\leqslant\eta\leqslant a\leqslant\xi. \tag{9}$$

The remaining octants are obtained from appropriate reflections. The (ξ,η,ζ)-coordinate surfaces are shown in Fig. 2. The boundary hyperboloid (1) (in scaled coordinates) coincides with the coordinate surface $\eta=1$, i.e., within the boundary hyperboloid η is restricted to $[b,1]$. The parameter b determines the asymmetry of the cross section of the constriction with $b=0$ leading to an axially symmetric constriction. The parameter a determines how strong the narrowness changes with z: for $a\to\infty$ the constriction becomes cylindrical with an elliptical cross section; for $a\to 1$ the constriction degenerates to the x-y plane with a hole having the shape of an ellipse.

Equality in one of the equations in (9) gives the Cartesian coordinate planes: $\zeta=0$ gives the y-z plane; $\zeta=b$ and $\eta=b$ give two surface patches which together cover the x-z plane; $\eta=a$ and $\xi=a$ give two surface patches which together cover the x-y plane; see Fig. 3(a). Considering only the region enclosed by the boundary hyperboloid (1), the coordinate planes $\xi=\text{const}\geqslant a$ are transverse to the z direction. Note that the singular coordinate plane $\xi=a$ is a region in the x-y plane which is enclosed by an ellipse which lies outside of the hyperboloidal constriction; see Fig. 3(b). The coordinate ξ thus parametrizes the direction of transmission; η and ζ parametrize the two directions transverse to transmission.

With the ansatz $\psi(\xi,\eta,\zeta)=\psi_\xi(\xi)\psi_\eta(\eta)\psi_\zeta(\zeta)$ the Helmholtz equation (4) can be separated and turned into the set of ordinary differential equations

$$-\left(\sqrt{(s^2-a^2)(s^2-b^2)}\frac{d}{ds}\right)^2\psi_s(s)=2E(s^4-2ks^2+l)\psi_s(s), \tag{10}$$

where $s\in\{\xi,\eta,\zeta\}$ and k and l are separation constants. The equations for ξ, η, and ζ are identical, but they have to be considered on the different intervals (9) and for different boundary conditions. In fact the equations have regular singular points[22] at $\pm a$ and $\pm b$. All the regular singular points have indices 0 and 1/2, i.e., there are solutions, which near $\sigma=\pm a$ or $\sigma=\pm b$ are of the form $\psi_s(s)=(s-\sigma)^{q_\sigma}\tilde{\psi}(s)$ where $\tilde{\psi}(s)$ is analytic and $q_\sigma=0$ or $q_\sigma=1/2$. As the elliptic coordinates (ξ,η,ζ) give for the regular singular points $\pm a$ and $\pm b$ the Cartesian x-z plane and x-y plane, respectively, the indices determine the parities π_y and π_z of the total wave function $\psi(\xi,\eta,\zeta)$.[23] In particular, $q_b=0$ or $q_b=1/2$ correspond to

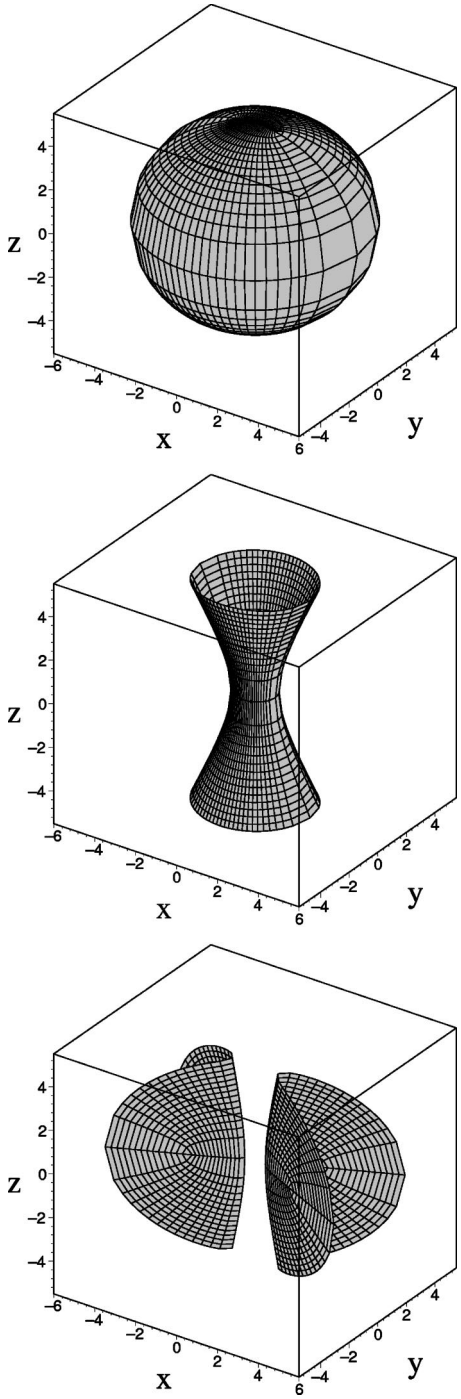

FIG. 2. Coordinate surfaces $\xi=5$ (top), $\eta=1$ (middle), and $\zeta=1/2$ (bottom). $[(a^2,b^2)=(5,0.2).]$

total wave functions which have $\pi_y=+$ or $\pi_y=-$, respectively.

To compute the transmission probabilities T_n we look for solutions of the form

$$\psi_{\xi;n}(\xi)\psi_{\eta;n}(\eta)\psi_{\zeta;n}(\zeta)+r_n\psi^*_{\xi;n}(\xi)\psi_{\eta;n}(\eta)\psi_{\zeta;n}(\zeta) \quad (11)$$

at the bottom $(z\ll -1)$ and

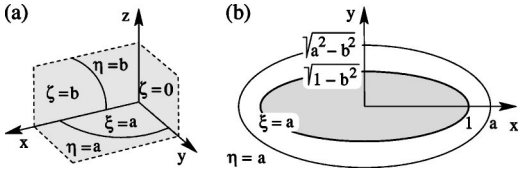

FIG. 3. (a) Singular elliptic coordinate surfaces. (b) "Bottleneck" (shaded region) in the x-y plane bounded by the hyperboloidal constriction whose intersection with the x-y plane is the ellipse $x^2/1+y^2/(1-b^2)=1$, and singular coordinate patches $\xi=a$ and $\eta=a$ [inside and outside of the ellipse $x^2/a^2+y^2/(a^2-b^2)=1$, respectively].

$$t_n\psi^*_{\xi;n}(\xi)\psi_{\eta;n}(\eta)\psi_{\zeta;n}(\zeta) \quad (12)$$

at the top $(z\gg 1)$. Such solutions can be computed from first solving the wave equations (10) for the transversal coordinates η and ζ and the corresponding boundary conditions with E as a parameter. The boundary conditions for ψ_η are given by the parity π_y which yields the index of ψ_η at $\eta=b$ and the Dirichlet boundary condition $\psi_\eta(1)=0$. The boundary conditions for ψ_ζ are determined by the parities π_y and π_x: π_y determines the index of ψ_ζ at $\zeta=b$ and π_x determines whether $\psi'_\zeta(0)=0$ $(\pi_x=+)$ or $\psi_\zeta(0)=0$ $(\pi_x=-)$. This defines modes which we label by the Dirac "kets" $|n_\eta,n_\zeta,\pi_x,\pi_y\rangle$ where n_η and n_ζ are non-negative quantum numbers which give the number of nodes of ψ_η and ψ_ζ in the open intervals $b<\eta<1$ and $0<\zeta<b$, respectively. The modes for energy E determine the separation constants $\mathbf{(}k_{(n_\eta,n_\zeta,\pi_x,\pi_y)}(E),l_{(n_\eta,n_\zeta,\pi_x,\pi_y)}(E)\mathbf{)}$. These are used in the equation for ξ in (10) from which the transmission probabilities $T_n=|t_n|^2$, with n being the set of quantum numbers n_ζ and n_η and parities π_x and π_y, are then given in terms of the asymptotic behavior of the resulting solutions ψ_ξ in the limit $\xi\to\infty$ (see, e.g., Ref. 24).

For the interpretation of the results below it is useful to remove the singularities in (10). This can be achieved by the transformation

$$(\xi(\lambda),\eta(\mu),\zeta(\nu))=a\left(\frac{\mathrm{dn}(\lambda,q)}{\mathrm{cn}(\lambda,q)},\mathrm{dn}(\mu,q'),\frac{b}{a}\mathrm{sn}(\nu,q)\right), \quad (13)$$

where $\mathrm{sn}(\phi,q)$, $\mathrm{cn}(\phi,q)$, and $\mathrm{dn}(\phi,q)$ are Jacobi's elliptic functions with "angle" ϕ and modulus q.[25] Here the modulus is given by $q=b/a$. $q'=(1-q^2)^{1/2}$ denotes the conjugate modulus. This is the standard parametrization of elliptic coordinates by elliptic functions.[22] To cover the positive (x,y,z) octant (λ,μ,ν) have to vary in the ranges

$$0\leqslant\lambda\leqslant\infty,\quad 0\leqslant\mu\leqslant K(q'),\quad 0\leqslant\nu\leqslant K(q), \quad (14)$$

where $K(q)$ and $K(q')$ are Legendre's complete elliptic integral of first kind with modulus q and q', respectively. The boundary hyperboloid (1) has

$$\mu_B=F([(a^2-1)/(a^1-b^2)]^{1/2},q') \quad (15)$$

which is Legendre's incomplete elliptic integral of the first kind with argument $[(a^2-1)/(a^1-b^2)]^{1/2}$ and modulus q'.

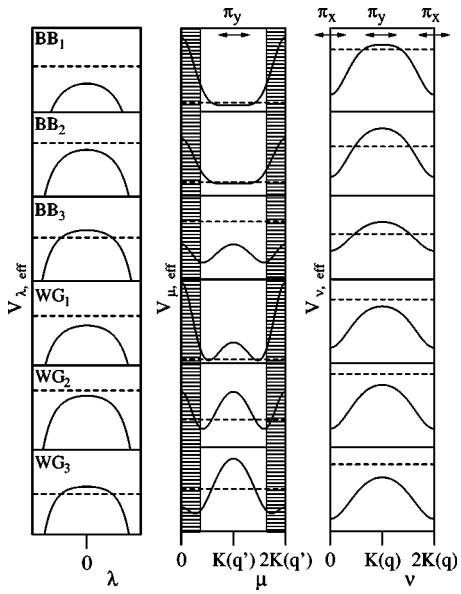

FIG. 4. Effective potentials and energies for constants of motions (s_1^2, s_2^2) [or equivalently (k,l)] in the regions BB_1, BB_2, BB_3, WG_1, WG_2, and WG_3 defined in Fig. 5 below. For the μ degree of freedom the hatched regions mark the forbidden regions $[0,\mu_B]$ and $[2K(q')-\mu_B, 2K(q')]$ which are not contained in the boundary hyperboloid (1). $[(a^2,b^2)=(3/2,1/2).]$

Transforming (10) to the coordinates (λ,μ,ν) leads to

$$-\frac{d^2}{d\hat{s}^2}\psi_{\hat{s}}(\hat{s}) = \sigma_{\hat{s}}\frac{2E}{a^2}[s(\hat{s})^4 - 2ks(\hat{s})^2 + l]\psi_{\hat{s}}(\hat{s}), \qquad (16)$$

where $\hat{s}\in\{\lambda,\mu,\nu\}$, $s(\hat{s})\in\{\xi(\lambda),\eta(\mu),\zeta(\nu)\}$ are the functions from Eq. (13) and the $\sigma_{\hat{s}}$ are the signs $\sigma_\lambda=\sigma_\nu=+$ and $\sigma_\mu=-$. Each of these equations can be interpreted as a one-dimensional Schrödinger equation with a Hamiltonian of the standard type "kinetic plus potential energy" with effective energy and potential

$$E_{\hat{s},\mathrm{eff}} = \sigma_{\hat{s}}\frac{E}{a^2}l, \quad V_{\hat{s},\mathrm{eff}}(\hat{s}) = -\sigma_{\hat{s}}\frac{E}{a^2}[s^4(\hat{s}) - 2ks^2(\hat{s})]. \quad (17)$$

The effective energies and potentials are shown for "representative" values of the separation constants k and l in Fig. 4 where μ and ν vary in intervals of length $2K(q')$ and $2K(q)$ which are the periods of the effective potentials $V_{\mu,\mathrm{eff}}$ and $V_{\nu,\mathrm{eff}}$, respectively. What we mean by "representative" will be explained in the following section where we analyze the corresponding classical system. The parities π_x and π_y at the top of Fig. 4 show how they determine the symmetry of the wave functions ψ_μ and ψ_ν at the various symmetry lines which correspond to the Cartesian coordinate planes: For $\pi_y=+/-$ the wave functions ψ_μ and ψ_ν are symmetric/asymmetric about $\mu=K(q')$ and $\nu=K(q)$, respectively. The wave function ψ_ν is symmetric/asymmetric about $\nu=0 \bmod 2K(q')$ for $\pi_x=+/-$. Though the algebraic equations (10) have (regular) singular points they are better suited for a numerical procedure than the equations in (16). The solutions are found from a shooting method which is explained in detail in Ref. 23.

III. CLASSICAL BILLIARD

For the calculation of the transmission probabilities T_n and their interpretation it is useful to consider the corresponding classical system. This is the (classical) billiard which consists of a mass which moves freely inside of the hyperboloidal boundary (1) and which becomes specularly reflected when it encounters the boundary. Like the quantum system the classical billiard can be separated in elliptic coordinates. The separated momenta conjugate to (ξ,η,ζ) can be written as

$$p_s^2 = 2E\frac{s^4-2ks^2+l}{(s^2-a^2)(s^2-b^2)} =: 2E\frac{(s^2-s_1^1)(s^2-s_2^2)}{(s^2-a^2)(s^2-b^2)}, \quad (18)$$

where $(s\in\{\xi,\eta,\zeta\})$, and $s_1^2=k-(k^2-l)^{1/2}$ and $s_2^2=k+(k^2-l)^{1/2}$ are the squares of the turning points of the motion in the respective coordinate direction. The analogous equations for the coordinates (λ,μ,ν) are

$$p_{\hat{s}}^2 = \sigma_{\hat{s}}\frac{2E}{a^2}(s^4(\hat{s}) - 2ks^2(\hat{s}) + l), \qquad (19)$$

where $\hat{s}\in\{\lambda,\mu,\nu\}$ and $s(\hat{s})\in\{\xi(\lambda),\eta(\mu),\zeta(\nu)\}$ are again the functions defined in (13). The specular reflection at the hyperboloidal boundary $\eta=1$ or $\mu=\mu_B$ becomes $(\xi,\eta,\zeta,p_\xi,p_\eta,p_\zeta)\mapsto(\xi,\eta,\zeta,-p_\xi,p_\eta,p_\zeta)$ or $(\lambda,\mu,\nu,p_\lambda,p_\mu,p_\nu)\mapsto(\lambda,\mu,\nu,-p_\lambda,p_\mu,p_\nu)$, respectively. Note that (18) and (19) are the classical analogs of the separated wave equations (10) and (16), respectively.

Expressing the separation constants k and l, or their energy scaled counterparts $K:=2Ek$ and $L:=2El$, in terms of Cartesian coordinates and momenta gives

$$K = \frac{1}{2}[|\mathbf{L}|^2 + (a^2+b^2)p_x^2 + a^2p_y^2 + b^2p_z^2], \qquad (20)$$

$$L = b^2L_y^2 + a^2L_z^2 + a^2b^2p_x^2, \qquad (21)$$

where L_x, L_y, and L_z denote the components of the angular momentum about the origin $\mathbf{L}=\mathbf{r}\times\mathbf{p}$. The separation constants together with the total energy $E=(p_x^2+p_y^2+p_z^2)/2$ give three constants of motion. Hence, the classical system is integrable.

The level set of each triple (E,k,l) defines an invariant set in the classical phase space. The invariant sets (generically) have the topology of Cartesian products of a line and two-tori $S^1\times S^1=T^2$ which we refer to as "toroidal cylinders" (as opposed to "pure" tori, which one finds in bounded integrable systems). Concerning the classical mechanics, the dependence on E can basically be ignored as E appears as a simple scaling factor for the momenta [see Eqs. (18) and (19)]. The physical ranges for k and l can be obtained from the disposition of the turning points s_1 and s_2 which is limited by the requirement that they simultaneously must yield real momenta in Eq. (18). It turns out that there are six different arrangements of the squared movable roots s_1^2 and s_2^2

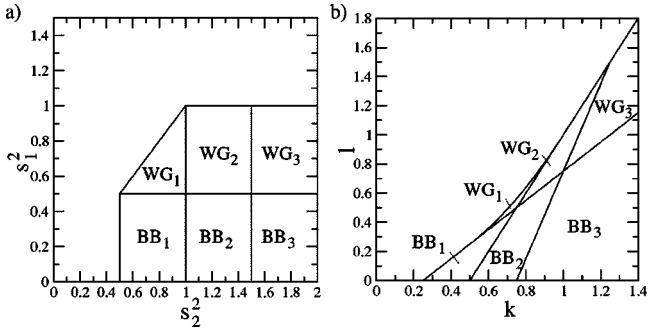

FIG. 5. Bifurcation diagram in terms of the variables (s_1^2, s_2^2) (a) and (k,l) (b). $[(a^2,b^2)=(3/2,1/2).]$

relative to the squared fixed roots a^2 and b^2. The six arrangements correspond to different types of motion or *phases*. We label the phases BB_1, BB_2, BB_3, WG_1, WG_2, and WG_3 as shown in the *bifurcation diagram* in Fig. 5.

For fixed energy E a pair (s_1^2, s_2^2) [or the corresponding pair (k,l)] in phase BB_1 or BB_2 has as its level set a toroidal cylinder $\mathbb{R}\times T^2$ which we illustrate in terms of its caustic, i.e., as the envelope of its projection to configuration space, in Fig. 6. It is unbound in the direction of ξ and the motion is oscillatory in the transverse degrees of freedom η and ζ. In phase BB_2 the motion oscillates with reflections at the boundary hyperboloid. In the elliptical cross section in the x-y plane the caustic of BB_2, which consists of two hyperbolas resulting from $\eta=s_1$, is that of the "bouncing ball modes" which one finds in the billiard in a planar ellipse.[26] In contrast to that the motion in phase BB_1, though oscillatory in η and ζ, does not touch the boundary hyperboloid, i.e., the corresponding toroidal cylinders are foliated by straight lines of free motions without reflections. A pair (s_1^2, s_2^2) in phase BB_3 represents motion which does not cross the x-y plane. The corresponding level sets consist of two toroidal "half cylinders" $(0,\infty)\times T^2$ which are bounded away from the x-y plane by the ellipsoid $\xi=s_2$.

Pairs (s_1^2, s_2^2) in phase WG_1 or WG_2 involve motions which are rotational in ζ (or, equivalently, in ν), they represent two toroidal cylinders $\mathbb{R}\times T^2$ which differ by the sense of rotation, see the corresponding panels in Fig 6. In the elliptical cross section in the x-y plane the caustic of WG_2, which is the ellipse resulting from $\eta=s_1$, is that of the "whispering gallery modes" which one finds in planar elliptic billiards. As in the case of BB_1, motions in phase WG_1 do not touch the hyperboloidal boundary. The corresponding toroidal cylinders are again foliated by lines of free motion without reflections. For (s_1^2, s_2^2) in phase WG_3 the rotational motions are again bound away from the x-y plane by the ellipsoid $\xi=s_2$. The corresponding level set consists of four toroidal half cylinders which have $z>0$ or $z<0$ combined with different senses of rotation.

The boundaries of the six phases correspond to critical motions. The corresponding level sets typically correspond to lower dimensional toroidal cylinders which might be stable or unstable.

IV. QUANTIZED CONDUCTANCE

As can be seen from the caustics in Fig. 6, the phases BB_1, BB_2, WG_1, and WG_2 are classically conducting; phases BB_3 and WG_3 are nonconducting. For constants of motion in phases BB_3 and WG_3 the motion cannot cross the x-y plane due to the presence of a *dynamical barrier*. This can be seen from the effective energy $E_{\lambda,\mathrm{eff}}$ which for phases BB_3 and WG_3 lies below the energy of the maximum of the effective potential $V_{\lambda,\mathrm{eff}}$ at $\lambda=0$; see the corresponding panels in Fig. 4.

Quantum mechanically it is possible to tunnel through this dynamical barrier. The tunnel probability is described by the tunnel integral

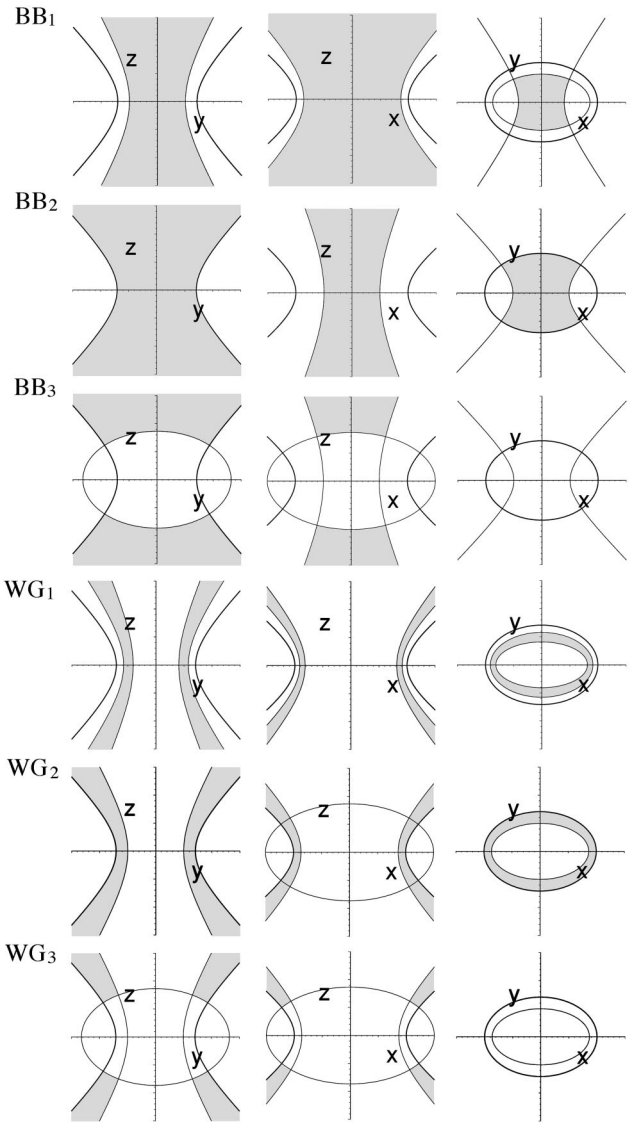

FIG. 6. Caustics of the six types of classical motions BB_1, BB_2, BB_3, WG_1, WG_2, and WG_3 as their intersections with the Cartesian coordinate planes. The caustics delimit the regions of the corresponding classical motions in configuration space which are shown as the shaded regions. The bold lines mark the intersections of the hyperboloidal boundary (1). The ranges for x, y, and z are $[-3/2,3/2]$. $[(a^2,b^2)=(3/2,1/2).]$

$$\Theta_{(n_\eta,n_\zeta,\pi_x,\pi_y)}(E)=i\int_{\lambda_-}^{\lambda_+}p_\lambda d\lambda=2i\sqrt{2E}\int_a^{s_2}\sqrt{\frac{\xi^4-2k_{(n_\eta,n_\zeta,\pi_x,\pi_y)}(E)\xi^2+l_{(n_\eta,n_\zeta,\pi_x,\pi_y)}(E)}{(\xi^2-a^2)(\xi^2-b^2)}}d\xi. \tag{22}$$

For $E_{\lambda,\mathrm{eff}}<V_{\lambda,\mathrm{eff}}(0)$ p_λ is imaginary along the integration interval which is bounded by the real classical turning points λ_- and $\lambda_+=-\lambda_-$. This integral can be identified with two times the integral of p_ξ from a to the corresponding turning point s_2 which gives the second equality in (22). For $E_{\lambda,\mathrm{eff}}>V_{\lambda,\mathrm{eff}}(0)$ the classical turning points $\lambda_\pm$ become imaginary (with λ_- complex conjugate to λ_+) whereas p_λ is real on the imaginary axis between $\lambda_\pm$. This corresponds to $s_2<a$ in the second integral in (22). The branch of the square root in (22) is chosen such that the tunnel integral is positive if $a<s_2$ and negative if $s_2<a$. This leads to a *uniform* transmission probability[24]

$$T_{(n_\eta,n_\zeta,\pi_x,\pi_y)}(E)=\frac{1}{1+\exp[2\Theta_{(n_\eta,n_\zeta,\pi_x,\pi_y)}(E)]}. \tag{23}$$

The resulting conductance which, up to a prefactor, is the sum over the $T_{(n_\eta,n_\zeta,\pi_x,\pi_y)}(E)$ for all quantum numbers n_η and n_ζ and parities π_x and π_y is shown in Fig. 7. Depending on the shape parameters (a^2,b^2) for the boundary hyperboloid the conductance shows more or less pronounced steps of the size of integer multiples of $e^2/(\pi\hbar)$.

A detailed analysis of the conductance curve can be obtained from relating the modes $|n_\eta,n_\zeta,\pi_x,\pi_y\rangle$ to the classical motions. For a given energy E this relationship is established via the separation constants $(k_{(n_\eta,n_\zeta,\pi_x,\pi_y)}(E),l_{(n_\eta,n_\zeta,\pi_x,\pi_y)}(E))$ which determine the toroidal cylinders and their caustics. The wave functions of the modes $|n_\eta,n_\zeta,\pi_x,\pi_y\rangle$ are mainly

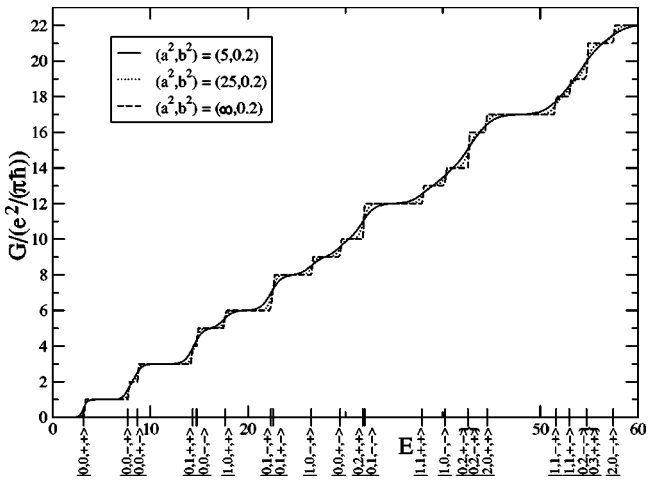

FIG. 7. Conductance as a function of energy [in units of $\hbar^2/(\tilde{c}^2m_e)$] for different shape parameters (a^2,b^2) of the hyperboloidal constriction. The limit $(a^2,b^2)=(\infty,0.2)$ corresponds to the conductance through a cylinder with an elliptical cross section. The ticks on the energy axis mark the energies at which, for $(a^2,b^2)=(5,0.2)$, the transition channels $|n_\eta,n_\zeta,\pi_x,\pi_y\rangle$ "open," see text.

"concentrated" on the projections of the corresponding toroidal cylinders to configuration space. As can be seen from their caustics in Fig. 6, for the whispering gallery phases, these projections become increasingly confined in the order $\mathrm{WG}_3\rightarrow\mathrm{WG}_2\rightarrow\mathrm{WG}_1$. For the bouncing ball phases the confinement increases in the order $\mathrm{BB}_3\rightarrow\mathrm{BB}_2\rightarrow\mathrm{BB}_1$. Since high confinement in configuration space implies high kinetic energy via the Heisenberg uncertainty principle, the modes, which classically correspond to the phases WG_1 or BB_1, have highest energy. In fact, for low energies all modes have $(k_{(n_\eta,n_\zeta,\pi_x,\pi_y)}(E),l_{(n_\eta,n_\zeta,\pi_x,\pi_y)}(E))$ in the classically nonconducting phases WG_3 or BB_3. Upon increasing the energy the $(k_{(n_\eta,n_\zeta,\pi_x,\pi_y)}(E),l_{(n_\eta,n_\zeta,\pi_x,\pi_y)}(E))$ wander toward the conducting modes WG_2 or BB_2, and for even higher energy to WG_1 or BB_1; see Fig. 5. Concerning the classical mechanics, the border between nonconductance and conductance is given by $s_2^2=a^2$ or $l=k^2-(a^2-k)^2$. This border is crossed for the modes $|n_\eta,n_\zeta,\pi_x,\pi_y\rangle$ for different energies. Upon crossing the border the tunnel integral changes sign and the transmission probability changes from 0 to 1. The energy for which the tunnel integral of a mode is zero can be defined as the energy at which the mode "opens" as a transmission channel. These energies are marked on the energy axis in Fig. 7.

Classically, the border $s_2^2=a^2$ corresponds to the unstable invariant motion in the x-y plane. This is the planar billiard in the bottleneck ellipse which is an invariant subsystem with one degree of freedom less than the full three-dimensional billiard.

Due to the dynamical barrier the wave functions of the modes deep in the nonconducting phases WG_3 and BB_3 have negligible amplitudes in the x-y plane. As the energy increases the increase of the amplitudes is indicated by the switching of the corresponding transmission probability $T_{(n_\eta,n_\zeta,\pi_x,\pi_y)}$ from 0 to 1, i.e., the "opening" of a new transmission channel. The wave functions of the transmission channels which lead to conductance step in Fig. 7 are shown in Fig. 9 below as their intersection with the x-y plane.

The quantum mechanical manifestation of the two senses of rotation in the whispering gallery phases is the energetic quasidegeneracy of the corresponding modes $|n_\eta,n_\zeta,\pi_x,\pi_y\rangle$. The further the separation constants $(k_{(n_\eta,n_\zeta,\pi_x,\pi_y)}(E),l_{(n_\eta,n_\zeta,\pi_x,\pi_y)}(E))$ in the whispering gallery phases lie away from the border $s_1^2=b^2$ to bouncing ball motions, the higher the effective energy $E_{\nu,\mathrm{eff}}$ lies above the effective potential $V_{\nu,\mathrm{eff}}$. In this limit the role of the potential becomes negligible and the energy is essentially determined by the total number of nodes of ψ_ν along a complete ν loop which is an ellipse in Fig. 9. The sum of the nodes in the four open Cartesian x-y quadrants plus possible additional nodes on $x=0$ or $y=0$ depending on the parities π_x and π_y gives the total number of ψ_ν nodes

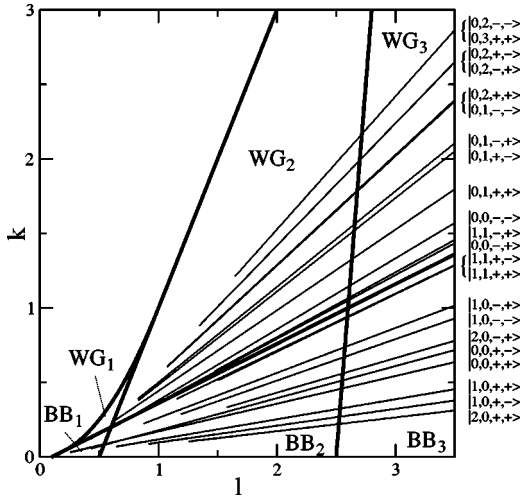

FIG. 8. The (k,l) spectra of the modes leading to the conductance jumps in Fig. 7 for $(a^2,b^2)=(5,0.2)$. For each shown mode $|n_\eta,n_\zeta,\pi_x,\pi_y\rangle$ the energy E is varied from 2 [for which $(k_{(n_\eta,n_\zeta,\pi_x,\pi_y)}(E),l_{(n_\eta,n_\zeta,\pi_x,\pi_y)}(E))$ are in the nonconducting phases BB_3 or WG_3 beyond the right border of the shown region] to $E=100$ for which $(k_{(n_\eta,n_\zeta,\pi_x,\pi_y)}(E),l_{(n_\eta,n_\zeta,\pi_x,\pi_y)}(E))$ are in one of the classically conducting phases BB_1, BB_2, WG_1, or WG_2. The bold lines mark the classical bifurcation diagram.

$$\text{no. of nodes of } \psi_\nu = 4n_\zeta + 2 - (\pi_x + \pi_y). \tag{24}$$

This leads to the energetic degeneracy of the two pairs of modes

$$|n_\eta,n_\zeta+1,+,+\rangle \leftrightarrow |n_\eta,n_\zeta,-,-\rangle, \tag{25}$$

$$|n_\eta,n_\zeta,+,-\rangle \leftrightarrow |n_\eta,n_\zeta,-,+\rangle. \tag{26}$$

In Fig. 7 this effect is seen for the pairs of modes $|0,1,+,+\rangle$ and $|0,0,-,-\rangle$, $|0,1,-,+\rangle$ and $|0,1,+,-\rangle$, $|0,2,+,+\rangle$ and $|0,1,-,-\rangle$, $|0,2,+,-\rangle$ and $|0,2,-,+\rangle$, $|0,2,-,-\rangle$ and $0,3,+,+\rangle$ which, on the energy axis, become more and more indistinguishable as energy increases, and this way effectively lead to conductance steps of $2e^2/(\pi\hbar)$. For the degeneracies (25) and (26) to occur both modes in each pair have to be of whispering gallery type. From Fig. 8 and the wave functions in Fig. 9 we see that this is indeed the case for all pairs just mentioned and that (25) and (26) do *not* lead to degeneracies if one or both modes are of bouncing ball type.

V. THE LIMITING CASE OF A CYLINDRICAL CONSTRICTION

In the limit $a\to\infty$ the hyperboloidal boundary (1) becomes a cylinder with an elliptical cross-section. The separated Helmholtz equations corresponding to the transverse degrees of freedom become the separated wave equations in a planar elliptic quantum billiard.[26] This is most easily seen from the wave equations in (10). We therefore define new variables $\rho=\mu+K(q')$ and $\phi=\nu+K(q)$ and new separation constants $\tilde{k}=k/a^2$ and $\tilde{l}=l/a^2$. Then, in the limit $a\to\infty$, the fourth-order term in (10) drops out and the equations for μ and ν become

$$-\frac{d^2}{d\rho^2}\psi_\rho(\rho) = -2E(-2\tilde{k}\cosh^2\rho+\tilde{l})\psi_\rho(\rho), \tag{27}$$

$$-\frac{d^2}{d\phi^2}\psi_\phi(\phi) = 2E(-2\tilde{k}\cos^2\phi+\tilde{l})\psi_\phi(\phi), \tag{28}$$

where we used that, for $a\to\infty$, $\eta(\rho+K(q'))=a\,\mathrm{dn}(\rho+K(q'),q')\to b\cosh(\rho)$ and $\zeta(\phi+K(q))=b\,\mathrm{sn}(\phi+K(q))\to b\cos\phi$ which are the standard parametrizations of elliptic coordinates in the plane in terms of (hyperbolic) trigonometric functions. For the constants of motion K and L in Eqs. (20) and (21) one finds $\tilde{K}:=K/a^2\to(p_x^2+p_y^2)/2$ and $\tilde{L}:=L/a^2\to L_z^2+b^2p_x^2$, i.e., $\tilde{K}$ reduces to the kinetic energy of the billiard in the planar ellipse and $\tilde{K}-2b^2\tilde{L}$ becomes $L_z^2-b^2p_y^2$, which is the product of the angular momenta about the focus points $(x,y)=(\pm b,0)$ and which gives the second constant of the motion in the planar elliptic billiard.

The dynamical barrier due to $V_{\lambda,\mathrm{eff}}$ becomes infinitely broad as $a\to\infty$. This leads to a suppression of quantum mechanical tunneling as indicated by a tunnel integral which changes rapidly from $-\infty$ to ∞ as E is varied. As a result the transmission probabilities $T_n(E)$ become "classical," i.e., they turn into step functions which change discontinuously from 0 to 1 at the respective critical energy which is determined by the quantization of the transversal degrees of freedom. In the limit of a cylindrical constriction the conductance becomes thus proportional to the integrated density of states $N(E)$ of an elliptic quantum billiard, i.e.,

$$G(E)=\frac{e^2}{\pi\hbar}N(E)=\frac{e^2}{\pi\hbar}\int_0^E\sum_n\delta(\tilde{E}-E_n)d\tilde{E} \tag{29}$$

where the E_n are the eigenenergies of an elliptic quantum billiard. The resulting conductance curve which has sharp conductance steps is also shown in Fig. 7. It is remarkable that the energies of the conductance steps depend only very weakly on a, i.e., on how the narrowness of the constriction changes along the direction of transmission. The deviation from the cylindrical constriction (finite a) only results in a smoothing of the conductance steps due to tunneling. Disregarding the tunneling, the conductance through the hyperboloidal constriction is thus essentially determined solely by the quantum spectrum of the planar billiard in the bottleneck ellipse.

VI. CONCLUSIONS AND OUTLOOK

In this work we have studied in detail both classically and quantum mechanically the three-dimensional ballistic electron transport through an asymmetric hyperboloidal constriction. Hyperboloidal constrictions give the most general class of constrictions which allow for a separation of the Helmholtz equation (and the corresponding classical problem) and hence for an explicit solution of the transmission problem. The asymmetry leads to the coexistence of two kinds of modes, "whispering gallery modes" and "bouncing ball modes." The whispering gallery modes are quasidegenerate in the sense that they open as transition channels in pairs of

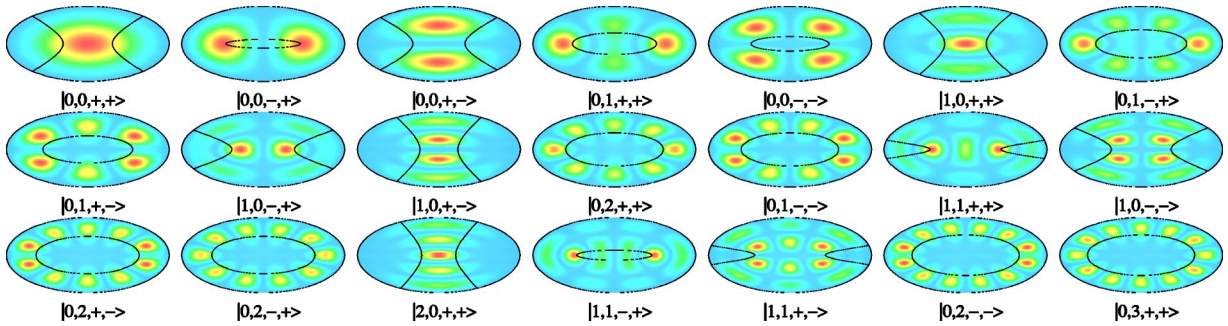

FIG. 9. (Color online) Probability contours in the section $z=0$ of the wave functions of the modes $|n_\eta, n_\xi, \pi_x, \pi_y\rangle$ at the moment when they "open" as transition channels (see text). The wave functions are displayed in the order they contribute to the conductance in Fig. 7. Light (blue) corresponds to low probability; dark (red) corresponds to high probability. The black lines mark the caustics of the classical motion. Ellipses indicate whispering gallery modes; hyperbolas indicate bouncing ball modes.

approximately the same energy. This way whispering gallery modes effectively lead to conductance steps of size $2e^2/(\pi\hbar)$ whereas bouncing ball modes give conductance steps of size $e^2/(\pi\hbar)$. Bouncing ball modes are a phenomenon of asymmetric constrictions and do not appear in the case of axially symmetric constrictions which have been discussed earlier by Torres, Pascual, and Sáenz.[18] In our study the axially symmetric case is contained as the limiting case $b\to 0$ [or equivalently $\tilde{b}\to\tilde{c}$ in the unscaled equation for the boundary hyperboloid in Eq. (1)] which leads to a vanishing of the bouncing ball phases; see the classical bifurcation diagram in Fig. 5. In the axially symmetric limit the quasidegeneracy of the whispering gallery modes becomes an exact degeneracy.

For non-vanishing temperature T the Landauer-Büttiker formula contains the Fermi-Dirac occupation probability. In this case Eq. (2) has to be replaced by

$$G(E)=\frac{e^2}{\pi\hbar}\sum_n \int \left(-\frac{\partial F}{\partial \tilde{E}}\right)_{\tilde{E}=E} T_n(\tilde{E})d\tilde{E}, \qquad (30)$$

where $F(\tilde{E})=1/\{1+\exp[(\tilde{E}-E)/(k_BT)]\}$ and the derivative is taken at the Fermi energy E. If T goes to zero the derivative turns into a δ function and we recover the conductance formula (2). A nonvanishing temperature thus leads to a smoothing of the conductance steps similar to the effect of tunneling.

Depending on the experimental setup it might be a better approximation to replace the hard-wall constriction considered in this and many other works (see, e.g., Refs. 14 and 17) by a smooth potential. The analog of transmission through a narrow constriction in a smooth system can be considered to be the transport across a potential saddle or, more generally, across a saddle-center (two degrees of freedom) or saddle-center-center (three degrees of freedom) equilibrium point. A saddle-center-$\cdots$-center is an equilibrium point at which the matrix of the diagonalization of the Hamiltonian vector field has one pair of real eigenvalues and otherwise imaginary eigenvalues. Transport across saddle-center-$\cdots$-centers is the mechanism for "transformation" in a large and diverse number of applications. It can be studied within the powerful framework of *transition state theory* which has its origin of conception in chemistry to compute reaction rates.[27] Ideas from transition state theory have been applied to a two-dimensional electron flow across a potential saddle by Eckhardt.[28] For a two degree-of-freedom system the classical flux (which gives the conductance) for an energy above that of the potential saddle is given by the action of an unstable periodic orbit of that energy; the Lyapunov periodic orbit associated with the saddle. The quantized conductance steps can be described in terms of the EBK quantization of this action. Recent developments in dynamical systems theory show how to generalize these ideas to an arbitrary (but finite) number of degrees of freedom.[29,30] These results show that, in the neighborhood of a saddle-center-$\cdots$-center equilibrium point, the dynamics is *generically* integrable. The unstable periodic orbit generalizes to a so-called *normally hyperbolic invariant manifold* (NHIM) which, for an degree-of-freedom system, has the topology of a $(2n-3)$-dimensional sphere. The NHIM is what in the chemistry literature is referred to as "activated complex;" an invariant system with one degree of freedom less than the full system located between "reactants" and "products."[31,32] The classical flux is given in terms of a generalized action integral over the NHIM.[33] Quantum effect on the flux can be described in terms of the EBK quantization of the invariant tori which foliate the NHIM.[34]

As hard-wall constrictions are often good models in the study of mesoscopic systems it is desirable to transfer the ideas from transition state theory to billiard systems. For the hyperboloidal constriction studied in this paper the NHIM consists of the unstable invariant subsystem which is the planar billiard in the bottleneck ellipse, which is located between "reactants" and "products" (the electron reservoirs at $z<0$ and $z>0$, respectively) and whose spectrum essentially determines the conductivity. Due to the normal hyperbolicity this invariant set persists under nonintegrable perturbations (this can be made precise in terms of the billiard map). But it is unclear how to compute the NHIM for a generic, i.e., nonseparable, hard-wall constriction in a three-dimensional electron gas. The computation of the NHIM is important as certain homoclinic orbits to the NHIM give rise to the existence of a high dimensional chaotic saddle which should have strong consequences for the conductivity.[35] Moreover,

heteroclinic connections between the NHIMs of a succession of narrow constrictions should provide a framework to study questions of additivity of resistance.[36] This will be the subject of future studies.

ACKNOWLEDGMENTS

The author acknowledges helpful discussions with Roman Schubert. This work was supported by the Deutsche Forschungsgemeinschaft (Wa 1590/1-1).

[1] R. M. Westervelt, M. A. Topinka, B. J. Leroy, A. C. Bleszynski, S. E. J. Shaw, S. E. J. Heller, K. D. Maranowski, and A. C. Gossard, Physica E (Amsterdam) **18**, 138 (2003).
[2] L. Olesen, E. Lægsgaard, I. Stensgaard, F. Besenbacher, J. Schiøtz, P. Stoltze, K. W. Jacobsen, and J. K. Nørskov, J. Phys.: Condens. Matter **72**, 2251 (1994).
[3] L. M. Krans, J. M. van Ruitenbeek, V. V. Fisun, I. K. Yanson, and L. J. de Jongh, Nature (London) **375**, 767 (1995).
[4] T. Ando, H. Matsumura, and T. Nakanishi, Physica B **323**, 44 (2002).
[5] G. Fiete and E. J. Heller, Rev. Mod. Phys. **75**, 933 (2003).
[6] A. Nitzan, Annu. Rev. Phys. Chem. **52**, 681 (2001).
[7] K. Richter and M. Sieber, Phys. Rev. Lett. **89**, 206801 (2002).
[8] A. S. Sachradja, R. Ketzmerick, C. Gould, Y. Feng, P. J. Kelly, A. Delage, and Z. Wasilewski, Phys. Rev. Lett. **80**, 1948 (1998).
[9] N. D. Lang, A. Yacoby, and Y. Imry, Phys. Rev. Lett. **63**, 1499 (1989).
[10] B. J. van Wees, H. van Houten, C. W. J. Beenakker, J. G. Williamson, L. P. Kouwenhoven, D. van der Marel, and C. T. Foxon, Phys. Rev. Lett. **60**, 848 (1988).
[11] D. A. Wharam, T. J. Thornton, R. Newbury, M. Pepper, H. Ahmed, J. E. F. Frost, D. G. Hasko, D. C. Peacock, D. A. Ritchie, and G. A. Jones, J. Phys. C **21**, L209 (1988).
[12] C. Rubio, N. Agraït, and S. Vieira, Phys. Rev. Lett. **76**, 2302 (1996).
[13] A. Stalder and U. Dürig, J. Phys.: Condens. Matter **68**, 637 (1996).
[14] C. A. Stafford, D. Baeriswyl, and J. Bürki, Phys. Rev. Lett. **79**, 2863 (1997).
[15] C. A. Stafford, F. Kassubek, J. Bürki, and H. Grabert, Phys. Rev. Lett. **83**, 4836 (1999).
[16] F. Kassubek, C. A. Stafford, and H. Grabert, Phys. Rev. B **59**, 7560 (1999).
[17] M. Yosefin and M. Kaveh, Phys. Rev. Lett. **64**, 2819 (1990).
[18] J. J. Torres, J. A. Pascual, and J. I. Sáenz, Phys. Rev. B **49**, 16 581 (1994).
[19] R. Landauer, IBM J. Res. Dev. **49**, 223 (1957).
[20] R. Landauer, Philos. Mag. **21**, 863 (1970).
[21] M. Büttiker, in *Nanostructured Systems*, edited by M. Reed (Academic Press, New York, 1992), p. 191.
[22] P. Morse and H. Feshbach, *Methods of Theoretical Physics* (McGraw-Hill, New York, 1953).
[23] H. Waalkens, J. Wiersig, and H. R. Dullin, Ann. Phys. (N.Y.) **276**, 64 (1999).
[24] M. V. Berry and K. E. Mount, Rep. Prog. Phys. **35**, 315 (1972).
[25] I. S. Gradshteyn and I. M. Ryzhik, *Tables of Integrals, Series, and Products* (Academic Press, New York, 1965).
[26] H. Waalkens, J. Wiersig, and H. R. Dullin, Ann. Phys. (N.Y.) **260**, 50 (1997).
[27] D. G. Truhlar and B. C. Garrett, Annu. Rev. Phys. Chem. **58**, 1622 (1984).
[28] B. Eckhardt, J. Phys. A **28**, 3469 (1995).
[29] S. Wiggins, L. Wiesenfeld, C. Jaffé, and T. Uzer, Phys. Rev. Lett. **86**, 5478 (2001).
[30] T. Uzer, C. Jaffé, J. Palacián, P. Yanguas, and S. Wiggins, Nonlinearity **15**, 957 (2002).
[31] W. H. Miller, J. Phys. Chem. A **102**, 793 (1998).
[32] P. Pechukas, Annu. Rev. Phys. Chem. **32**, 159 (1981).
[33] H. Waalkens and S. Wiggins, J. Phys. A **37**, L435 (2004).
[34] H. Waalkens, A. Burbanks, and S. Wiggins, J. Chem. Phys. **121**, 6207 (2004).
[35] H. Waalkens, A. Burbanks, and S. Wiggins, J. Phys. A **37**, L257 (2004).
[36] D. A. Wharam, M. Pepper, H. Ahmed, J. E. F. Frost, D. G. Hasko, D. C. Peacock, D. A. Ritchie, and G. A. Jones, J. Phys. C **21**, L887 (1988).